periodica polytechnica

Civil Engineering
58/3 (2014) 243–253
doi: 10.3311/PPci.7329
http://periodicapolytechnica.org/ci

RESEARCH ARTICLE

Plastic Hinge Length of RC Columns under the Combined Effect of Near-Fault Vertical and Horizontal Ground Motions

Alireza Mortezaei
Received 2013-02-03, accepted 2014-02-28

Abstract

Plastic hinges are an extension of the ductile design concept used in building seismically resistant structures. The formation of a plastic hinge in an RC column in regions that experience inelastic actions depends on the characteristics of the earthquakes as well as the column details. Recordings from recent earthquakes have proved that in the near-fault region of large earthquakes, the vertical component of the near-fault ground motion has exceeded the horizontal, and damage to the structures has been predominantly by these motions. Therefore, this paper focuses on near-fault ground motions that have been recorded within rather 20 km of the causative fault and 936 inelastic time-history analyses have been performed to predict the nonlinear behavior of RC columns subjected to combined effect of near-fault vertical and horizontal ground motions. The effects of some parameters are evaluated analytically by finite element methods and the results are compared with corresponding experimental data. Findings from this study provide a simple expression to estimate plastic hinge length of RC columns subjected to the combined effect of near-fault vertical and horizontal ground motions.

Keywords

Plastic hinge length · vertical motion · near-fault ground motion · RC column

Alireza Mortezaei
Department of Civil Engineering, Semnan Branch, Islamic Azad University, Semnan, Iran
e-mail: a.mortezaei@semnaniau.ac.ir

Notation

A_g	gross area of section
A_s	area of tension reinforcement
c	distance from extreme compression fiber to neutral axis
d	effective depth of beam
f'_c	compressive strength of concrete
f_y	yield stress of reinforcement
h	overall depth of column
H	distance from critical section to point of contraflexure
L	column height
l_p	plastic hinge length
M_{cr}	bending moment at cracking
M_y	bending moment at yield
M_u	bending moment at ultimate
M_W	earthquake magnitude
P	applied axial force
P_0	nominal axial load capacity
Δ_u	ultimate displacement
Δ_y	yield displacement
φ	curvature
φ_{cr}	cracking curvature
φ_y	yield curvature
φ_u	ultimate curvature
θ	rotation
θ_e	elastic rotation
θ_p	plastic rotation
θ_t	total rotation
ρ_l	longitudinal reinforcement ratio
ρ	mass density
E	modulus of elasticity
ν	poisson's ratio

1 Introduction

Following a seismic activity, the ground moves in all directions and each direction of movement gives information about an earthquake. P waves are the first and fastest wave that is recorded, therefore, peak vertical ground motion take place earlier than peak horizontal motion. P waves are compressive and

travel upward through the body of the earth, so have a strong vertical component.

In the near-fault region of large earthquakes, the characteristics of strong ground motions change. Time durations become considerably shorter [1,2], velocity and displacement time histories can increase notably and become more pulse like. Recently there has been an increase in interest about vertical ground motions, because buildings have become more architecturally unique and more structurally complicated. It is well-known that vertical ground motions are high-frequency motions. The increase in axial force demands with a decrease in vertical period (increase in frequency) is in accordance with the high-frequency characteristic of vertical ground motions.

In many seismic design specification, for example in Iranian Earthquake Code [3], the effect of vertical ground motion is disregarded because the vibration mode of buildings are predominant in the horizontal direction, and the amount of vertical ground motion is small compared to that of the horizontal component. According to the large number of available studies, it is concluded that vertical shaking rise the axial column force, cause an increase in the moment and shear demand, and intensify plastic deformation, extend plastic hinge formation and finally reduce the ductility capacity of structural component. As a result, for design and specially for the detailing of critical regions, a good parameter is the required plastic hinge length. Inclusion of vertical ground motion has a significant influence on this parameter.

2 Research significance

The correspondence of fundamental period of the structure with the predominant periods of vertical ground motion leads to the major amplification of forces particularly on vertical load carrying members. That means, the major effect of the vertical ground motion on the building is to increase the axial demand on the vertical load carrying member. This amplification is significant for upper floor rather than for lower floors. Since the shear capacity of the column depends upon the axial demand, an increase in the axial force demand in the column results in an increase in the shear capacity of the column. It is useful for the seismic behavior of the column. However, a decrease in the axial force demand on the column results in a decrease in the shear capacity of the column. Vertical ground motion can force column into tension for short durations of time, thus reducing the column's shear capacity to just the shear strength of the transverse reinforcement. This may lead to the failure of the structure.

The evidence show that neglecting vertical component of the ground motion lead to serious underestimation of the demand, over-estimation of the capacity and thus endanger overall structural safety. Accordingly, this paper focuses on near-fault ground motions that have been recorded within 20 km of the causative fault; since, these ground motions were observed to possess significant vertical components. Firstly, this paper addresses the conditions leading to the vertical component having a significant effect on the response of RC columns. Then, findings from this study provide a simple expression to estimate plastic hinge length of RC columns subjected to the combined effect of near-fault vertical and horizontal ground motions.

3 Definition of plastic hinge length

Plastic hinges are an extension of the ductile design concept used in building seismically resistant structures. Energy is dissipated through the plastic deformation of specific zones at the end of a member without affecting the rest of the structure. The basic ideas of the incremental plasticity theory and the principles of limit analysis were first recognized and applied by Kazinczy [4]. Numerous techniques and models are available to estimate the plastic hinge length of RC members as described below.

3.1 Analytical method

The moment-curvature characteristics of a given cross-section can represent the deformation properties of an RC section. As can be seen from Fig. 1, the schematic moment-curvature curve of an RC member that fails after flexural yielding consists of three stages. Typically, point $A_{cracking}$ indicates the cracking point where the concrete starts to crack (φ_{cr} and M_{cr}). In the initial stages ($M < M_{cr}$), the response is elastic and linear. With an increase in the applied moment, cracking of concrete reduces the flexural rigidity of the section, the extent of which depends on the amount of reinforcement. At the higher load level, corresponding to point $B_{yielding}$, the tension steel begins to yield (φ_y and M_y), which is followed by the crushing of concrete at point $C_{crushing}$ (φ_u and M_u). A large increase in curvature and ductility normally occurs beyond the yield limit.

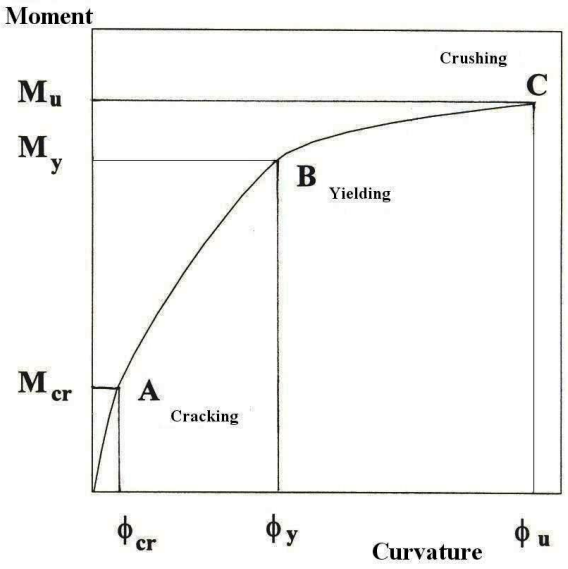

Fig. 1. Qualitative moment-curvature relationship

Rotation of a member can be determined from curvature distribution along the member length. Based on the conventional

structural engineering rules, the rotation (change of slope) between any two points is equal to the area under the curvature diagram between these two points. This is given by

$$\theta_{AB} = \int_{A}^{B} \varphi \, dx \tag{1}$$

where x is the distance of element dx from A. This equation can be applied whether elastic or inelastic curvatures are involved.

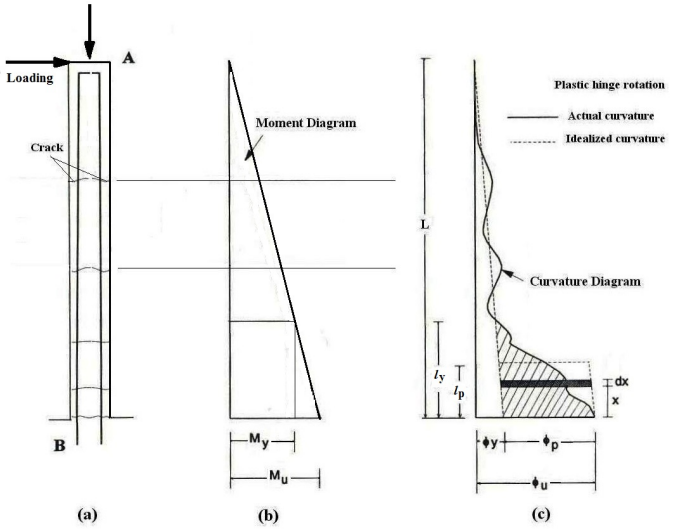

Fig. 2. Schematic curvature distribution along RC member at ultimate stage: (a) RC member, (b) bending moment diagram, (c) curvature diagram

The condition at the ultimate load stage of an RC member is shown in Fig. 2. For values of loads smaller than the yield moment, M_y, the curvature increases gradually from the free end of the member (point A) to the support (point B). There is a large increase in curvature at first yield of the tension steel. At the ultimate load stage, the curvature at the support increases suddenly, so that it causes a large inelastic deformation. Since the concrete between the cracks can carry some tension (tension-stiffening), the curvature fluctuates along the member length. Each of the peaks of curvature corresponds to a crack location. The actual distribution of curvature at the ultimate load level can be idealized into elastic and inelastic (plastic) regions (Fig. 2c); thus the total rotation, θ_t, over the member length can be divided into elastic, θ_e, and plastic, θ_p, rotations. The elastic rotation, θ_e, (until yielding of steel) can be obtained using the curvature at yield (Eq. (1)). According to Eq. (1), the plastic rotation can be determined, on each side of the critical section, as [5]:

$$\theta_p = \int_{0}^{l_y} \left|\varphi(x) - \varphi_y\right| \, dx \tag{2}$$

in which $\varphi(x)$ is the curvature at a distance x from the critical section at the ultimate load stage. The yielding length, l_y, is defined as the length of the member segment over which the maximum moment exceeds the yield moment, M_y, or the distance between the critical section and the location where the tension steel first yields (Fig. 2).

The shaded area in Fig. 2 is the plastic (inelastic) rotation, θ_p, which occurs in addition to the elastic rotation of the plastic hinge at the ultimate load stage. The plastic hinge rotation can be determined either by calculating the size of the shaded area or by an equivalent rectangle of height ($\varphi_u - \varphi_y$) and width l_p. Using Eq. (2), the equivalent plastic hinge length, l_p, can be defined as [5]:

$$l_p = \frac{1}{\left(\varphi_u - \varphi_y\right)} \int_{0}^{l_y} \left[\varphi(x) - \varphi_y\right] \, dx \tag{3}$$

Therefore, the value of plastic hinge rotation, θ_p, at the ultimate stage can be calculated using the following well-known equation:

$$\theta_p = (\varphi_u - \varphi_y) l_p = \varphi_p l_p = \beta' \varphi_p l_y \tag{4}$$

where φ_u and φ_y are the curvatures at the ultimate load and yield load, respectively, and l_p is the equivalent length of the plastic hinge over which the plastic curvature, ($\varphi_p = \varphi_u - \varphi_y$), is assumed to be constant. Eq. (4) results in the same area as the actual plastic curvature distribution (shaded area in Fig 2c). The dimensionless factor, β', is a shape factor or curvature distribution factor for the curvature diagram near the support and is less than 1. It may be called a reduction factor applied to the yielding length over which the steel reinforcement yields, so that $\beta' l_y = l_p$.

On the other hand, Iványi [6] introduced the concept of the interactive hinge and zone that take the changes developing in the load-displacement of the member. The interactive plastic hinge constitutes the extension and generalization of the traditional plastic hinge while the interactive zone that of the plastic zone.

3.2 Experimental method

Beam tip displacement test data from reversed cyclic loading of beam-column joint specimens have been used to determine the real plastic hinge lengths [7]. From force-displacement and moment-curvature test results, bilinear elastic perfectly plastic models have been used to obtain the yield and ultimate values of φ_y, φ_u, Δ_y and Δ_u. In order to determine the equivalent bilinear curve for the test results, the area under the curve (force-displacement or moment-curvature) is calculated, and a line having the initial slope of the curve is then drawn through the origin. Next, a horizontal line is drawn such that the area under the two lines is equal to the area under the original curve. The yield displacement/curvature is then defined as the point of intersection between the two lines and the ultimate value is considered as the maximum value of the displacement/curvature in the inelastic range. Eq. (5) and Eq. (6) can be solved to determine the value of l_p.

$$\Delta_p = \Delta_u - \Delta_y \tag{5}$$

$$\Delta_p = \left(\varphi_u - \varphi_y\right) l_p \left(L - 0.5 \cdot l_p\right) \tag{6}$$

where Δ_y and Δ_u represent the yield and the ultimate column tip displacement from test data, respectively.

Numerous models are available as empirical equations to estimate l_p for RC members. Many of these models consider a proportional increase of l_p with an increase of member length, depth and longitudinal reinforcement dimensions. Comparison between some popular expressions to estimate the plastic hinge length are presented in the next section.

4 Past studies

Previous studies in the literature are mainly focused on modeling and the effects of horizontal ground motions, whereas vertical earthquake effects has generally been neglected or underestimated in analysis and design.

Broderick and Elnashai [8] performed a 3D nonlinear analysis of a highway bridge in order to evaluate the critical response parameters. The vertical ground motion was found to cause fluctuation of pier axial load, therefore undermining shear capacity.

Abdelkareem and Machida [9] found that vertical motion caused change of final failure collapse of RC piers from flexural to severe diagonal shear failure. They concluded that the severity of diagonal collapse is higher in case of horizontal and vertical motions than that of only horizontal motions.

An evaluation of the characteristics of response spectra of free-field vertical motions recorded during the 1994 Northridge earthquake by Bozorgnia and Campbell [10] found the vertical to horizontal response spectral ratios to be strongly dependent on period and site-to-source distance. Kunnath and Zhao [11] investigated the effects of vertical ground motions on the seismic response of ordinary highway bridges. They concluded that vertical effects lead to significant variations in axial force demand in columns which can result in changes to moment and shear capacity of the column.

Kunnath et al. [12] examined a two-span highway bridge. It was found that vertical component of ground motion causes significant amplification in axial force demands in columns and moment demands in girders at both the midspan and the face of the bent cap. Hashemi and Abbasi [13] showed that ASCE standard overestimate the displacement of buildings and the vertical component of earthquake has no significant effect on the maximum displacement of stories. It was observed that using the ASCE equation for considering the vertical component of earthquake in far-fault areas can lead to an overestimation of axial force of columns, but in near-fault areas it can lead to a rather good estimation of axial force of columns.

Matsuzaki and Kawashima [14] carried out dynamic response analysis to evaluate the effects of predominant vertical ground motion on the seismic performance of an RC bridge. It was found from the analysis that the high vertical acceleration can result in immediate tension in addition to high compression pulses in the bridge pier due to resonant response in the vertical direction.

Kim et al [15] assess the effect of vertical component of ground motions on RC bridge piers. They reported that the inclusion of the vertical earthquake ground motion has an important effect on the response at all levels and components. As the V/H ratio (ratio of vertical to horizontal peak ground acceleration) increases, significant increases in axial force variation are observed. It was observed that the significant increase of axial force variation due to vertical ground motion leads to an observed reduction of shear capacity.

The plastic hinge length, l_p, of RC members depends on a number of parameters, including the definition of yielding and ultimate curvatures, section geometry, material properties, compression and tension reinforcement, transverse reinforcement, cracking, tension-stiffening and bond-slip characteristics between concrete and the reinforcing steel, the stress-strain curve for the concrete in tension and compression, the stress-strain curve for steel, support conditions and the magnitude and type of loading, axial force, width of the loading plate, influence of shear, and the presence of column as well as different characteristics of earthquakes.

Various expressions recommended for use in l_p estimations. A comparison of some reported l_p expressions is provided in Fig. 3, where it can be seen that the analytical value of l_p is not constant for the different values of the tension reinforcement indices.

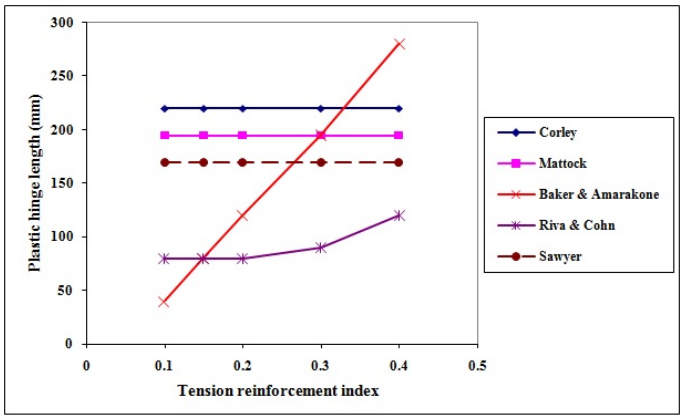

Fig. 3. Comparison of different equations for plastic hinge length

Baker's equation [16] gives a constant value of l_p equal to 194.5 mm (0.77 d) for different amounts of reinforcement index (ω). In contrast, in the latest equation proposed by Baker and Amarakone [17], l_p increases linearly with the c/d ratio. Riva and Cohn's formulation [18] results in the lowest values of plastic hinge length. The methods of Corley [19], Mattock [20], and Sawyer [21] give constant plastic hinge lengths, regardless of the reinforcement index, of 215.4 mm (0.85 d), 196.9 mm (0.78 d), and 168.2 mm (0.66 d), respectively. Fernandes et al. [22] investigated the cyclic behavior of a two-span RC beam built with plain reinforcing bars, collected from an ancient building structure. The beam displayed a flexural failure and the cracks were concentrated around the plastic hinges region. Cracks did not spread along the element's span. Instead, their width increased significantly during the test. They concluded that poor bond in-

fluences the plastic hinges length by reducing its value. It is interesting to note that most of the l_p expressions do not consider axial load as a parameter. More recently, Bae and Bayrak [23] and Mortezaei and Ronagh [24] showed that the level of axial load may influence the length of plastic hinges. Specimens tested by Bae and Bayrak [23] under high axial loads developed longer plastic hinges than those tested under low axial loads. They tested full-scale concrete columns under moderate to high axial load levels and reversed cyclic displacement excursions.

On the other hand, the large increases in the axial compression in columns due to vertical accelerations can lead to significant increases in the column moment capacity. Although this may suggest conservatism in the design, it may result in the shifting of the potential plastic hinge zone from the top of the column to the girder which is an undesirable situation. Therefore, an investigation into the l_p of reinforced concrete columns is needed to:

1 reconcile differences encountered in the previous research; and

2 develop an expression that can be used to estimate l_p more accurately under the combined effect of near-fault vertical and horizontal ground motions.

5 Characteristics and database of near-fault ground motions

The vertical component of the ground motion is associated with vertically propagating the P-waves and the wave-length of these waves are shorter than the other waves. It means frequency content of the vertical component of the ground motion is higher than the horizontal component. As can be seen in Fig. 4, the higher frequency content of the vertical component of the ground motion result in higher V/H ratio. Although the content over the first part of frequency range of the vertical ground motion is lower than that of the horizontal component, it has tendency to focus all its energy in narrow high frequency band. This high frequency content leads to largest response in short period range and cause significant response amplification.

Past studies recommend that the sites located within rather 20 Km from the major active fault should be designed to the combined effect of horizontal and vertical ground motion [25]. As a result, the ground motion database compiled for nonlinear time-history (NTH) analyses constitutes a representative number of near-fault ground motions from a variety of tectonic environments. A total of 7 records were selected to cover a range of frequency content, duration and amplitude. These records come from earthquakes having a magnitude (M_W) range of 6.2 to 7.3, and were recorded at closest fault distance of 0.0 to 7 km. Information pertinent to the ground motion data sets, including station, components of earthquake and peak ground acceleration (PGA) of vertical and horizontal components are presented in Table 1. The comparison of response spectrum of selected records have been shown in Fig. 5 and Fig. 6. The study of

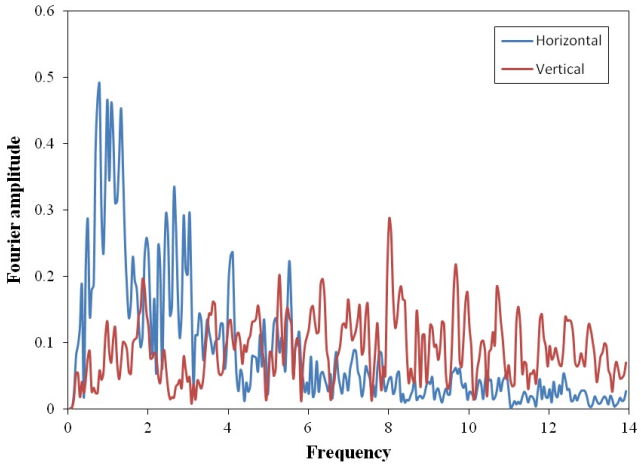

Fig. 4. Comparison of Fourier spectra of vertical and horizontal ground motion

these near-fault earthquake records indicates that: (a) the predominant period of the vertical ground motions are smaller than the corresponding horizontal component (Fig. 7); (b) the ratio of vertical-to-horizontal PGA decreases gradually with increasing fault distance, therefore, the vertical component of ground motions will be more severe for near fault ground motions.

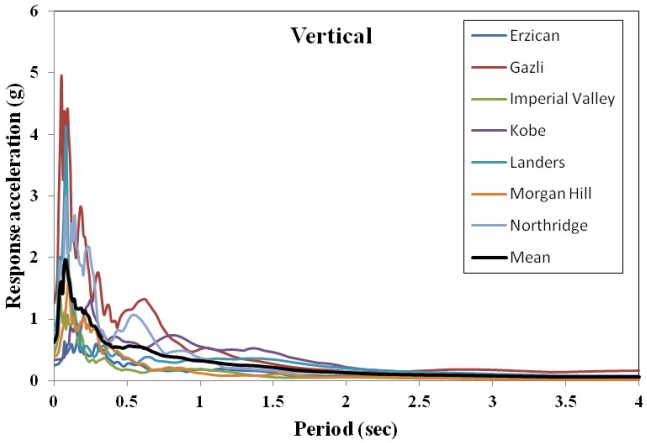

Fig. 5. Respone spectrum of vertical component of selected near-fault ground motions

Utilized in this study is a data processing technique proposed by Iwan et al. [26] and refined by Iwan and Chen [27] to recover the long period components from near-fault accelerograms. This process has been elaborated in Boore [28] and Boore et al. [29].

6 Verification of analytical models

The capability and accuracy of the finite element program and analytical models in predicting the nonlinear response of RC columns is verified along with a comparison between the analytical and corresponding experimental results. Kumagai and Kawashima [30] tested four full-scale columns with a 400 mm x 400 mm square cross sections as shown in Fig. 8 under the high frequency vertical ground motions at the Tokyo Institute of Technology, Japan. The height from the column base to loading point was 1.35 m. Longitudinal bars with a diameter

Tab. 1. Near-fault ground motion database

	Earthquake	Year	Station	Distance (km)	M_w	PGA-H_{max} (g)	PGA-H_{min} (g)	PGA-V_{ert} (g)
1	Gazli (USSR)	1976	Karakyr	5.46	7.1	0.718	0.608	1.264
2	Imperial Valley	1979	Bonds Corner	2.68	6.4	0.755	0.588	0.425
3	Morgan Hill	1984	Coyote Lake Dam	0.30	6.2	1.298	0.711	0.388
4	Erzican (Turkey)	1992	Erzincan	4.38	6.8	0.515	0.496	0.248
5	Landers	1992	Lucerne	2.19	7.3	0.785	0.721	0.818
6	Northridge	1994	Rinaldi Rec Stn	6.50	6.7	0.838	0.472	0.852
7	Kobe (Japan)	1995	KJMA	0.96	6.9	0.821	0.599	0.343

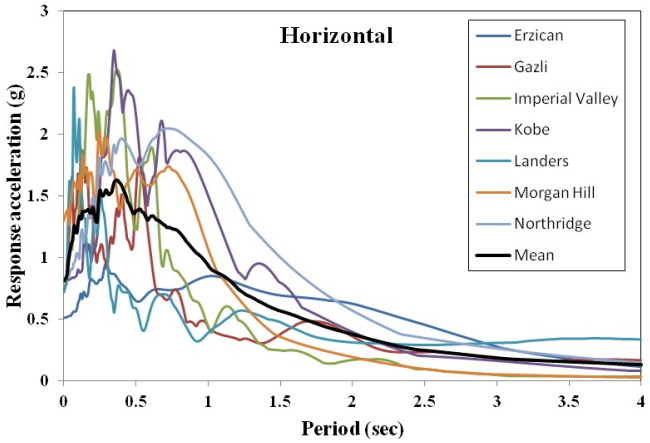

Fig. 6. Respone spectrum of horizontal component of selected near-fault ground motions

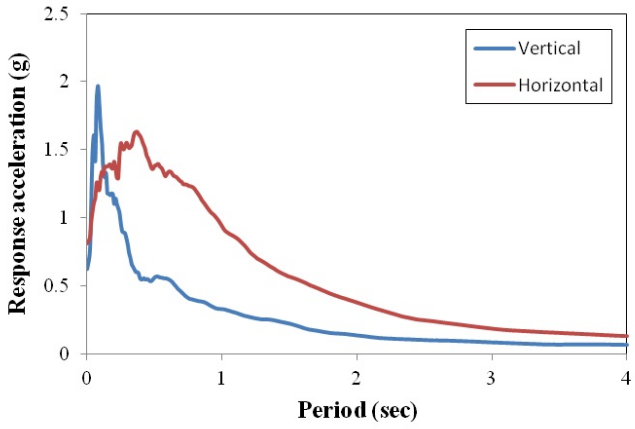

Fig. 7. Mean value comparison of response spectrum of selected near-fault records

of 13 mm and ratio of 1.58 % were set. Deformed tie bars with diameter of 6 mm were provided at 50 mm interval. Volumetric tie reinforcement ratio was 0.79 %. The columns were tested under the cyclic lateral displacement and vertical force. In the experiment, two combinations of vertical force and lateral displacement were considered. The frequency of varying vertical force was 0.15 Hz, which was 10 times to that of the lateral displacement, because the period of vertical force was 10 times shorter than that of the lateral displacement in the result of the preliminary dynamic response analysis of the selected column.

The column, plates, and supports were modeled as volumes. The combined volumes of the concrete and reinforcing bars are shown in Fig. 9. Fig. 9 illustrates that the rebar shares the same nodes at the points of intersection with the shear stirrups. The meshing of the reinforcement is a special case compared to the volumes. No meshing of reinforcement is needed because individual elements were created in the modeling through the nodes created by the mesh of the concrete volume.

The goal of the comparison in between the finite element (FE) model and the experimental work is to ensure that the model including its elements, material properties, real constants and convergence criteria is adequately simulating the response of the member. The shear force-lateral displacement hysteresis curve of the analytical model and the experimental work is shown in Fig. 10. The peak computed lateral force has good agreement with peak measured lateral force. The results indicate that FE program provides reasonable results and as such can be used to approximate the nonlinear behavior of RC columns under dynamic loading.

7 Parametric study

In this section, several inelastic time-history analyses have been performed in order to predict the plastic hinge length of RC columns using a FE program, and the results are compared with the corresponding experimental data. The FE program is

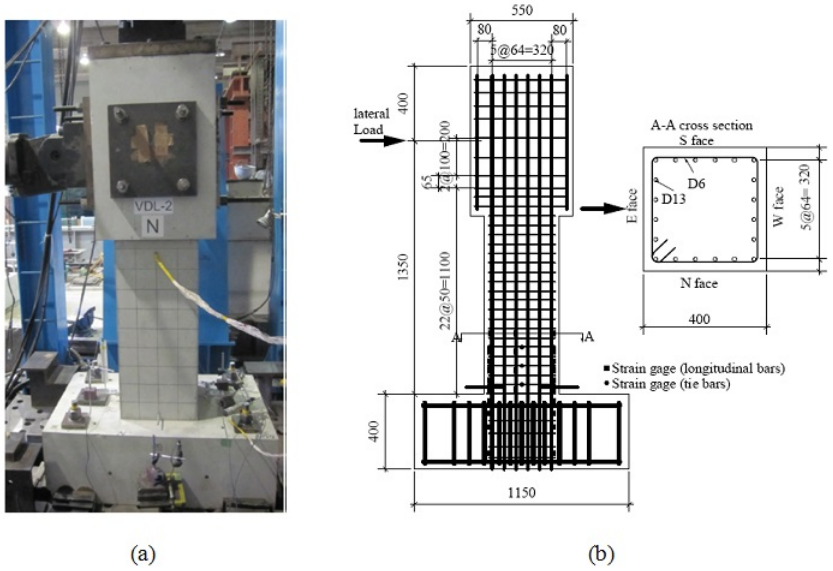

Fig. 8. (a) Column section and meshing in FE program; (b) reinforcement layout of analytical model

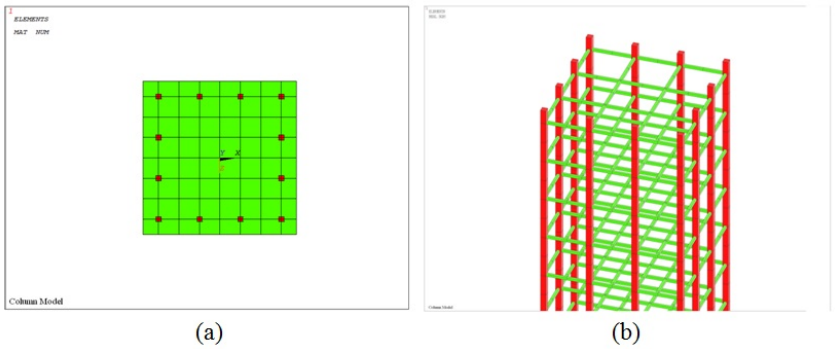

Fig. 9. (a) Column section and meshing in FE program; (b) reinforcement layout of analytical model

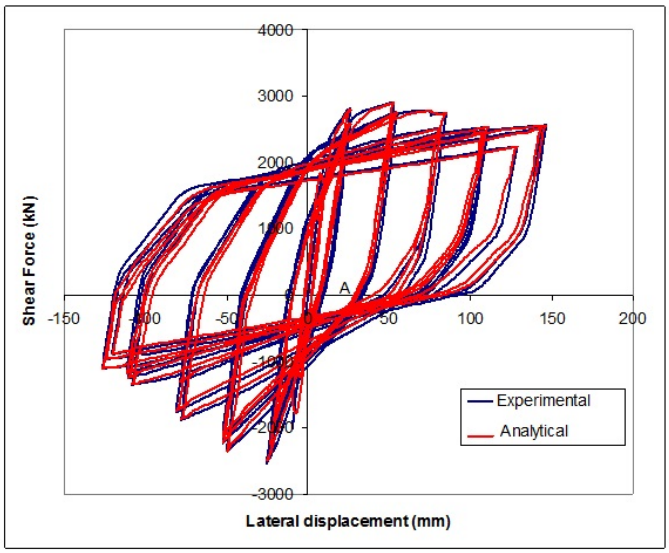

Fig. 10. The shear force-lateral displacement hysteresis curve of numerical model and experimental work

capable of predicting large displacement behavior of structures, taking into account both geometric nonlinearities and material inelasticity. The fiber modeling approach has been employed to represent the distribution of material nonlinearity along the length and cross-sectional area of the member.

The advantage of this approach is that the yielding length and the exact value of plastic rotation (shaded area in Fig. 2) can be determined without using the idea of equivalent plastic hinge length. Fig. 2 illustrates how the analytical plastic rotation and the equivalent plastic hinge lengths are determined. In summary, first, the curvature along the member is obtained from the concrete strain in the compression zone and from the steel strain in the tension zone at the ultimate state. Then, the plastic rotation is obtained by integration, along the yielding length (where the curvature in the section is higher than its yielding curvature), which is the length between the positions of ultimate curvature and yielding curvature. Finally, the equivalent plastic hinge length is calculated from that plastic rotation.

Using the above method, the influence of various parameters (axial load level (P/P_0), height-depth ratio (H/h), and strength of concrete, on l_p under the combined effect of near-fault vertical and horizontal ground motions are studied.

In the analysis, the modulus of elasticity (Young's modulus)

E = 30 kN/mm^2, Poisson's ratio ν = 0.20 and the mass density ρ = 24 kN/m^3 are assumed in all models. The uni-axial strength for nonlinear modeling of the concrete is considered variable. The rebar is modeled as steel with a yield strength of 400 Mpa and an ultimate strength of 600 Mpa.

7.1 Axial load level

The significant influence of fluctuations in the axial force demand of the columns can be the variation in the shear capacity of the columns. It is well known that the shear capacity of concrete depends on the axial force demand. An increase in the axial force demand in the column such as the one imposed by the vertical components of near-fault ground motions results in an increase in the shear capacity of the column which is beneficial to the seismic behavior of the column.

In this regard, to study the effect of axial load on the length of plastic hinge under near-fault earthquakes, 220 nonlinear dynamic analyses are conducted. The square RC columns with various levels of axial load under the 7 selected records are studied. The percentage of longitudinal reinforcements and height over depth ratios are kept constant at 1 % ($\rho_l = 0.01$) and 5 ($H/h = 5$), respectively. Table 2 and Fig. 11 illustrate the results of the analyses.

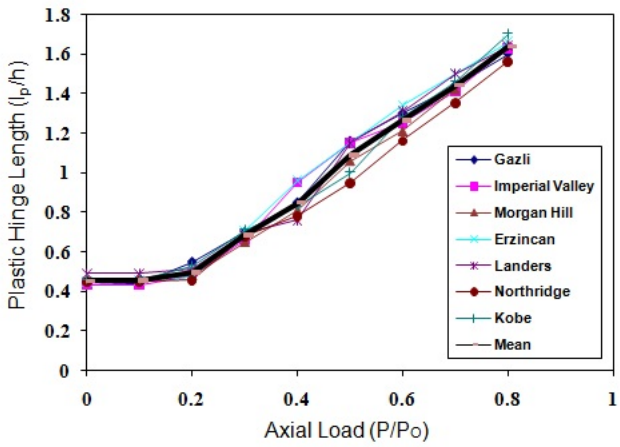

Fig. 11. Relationship between plastic hinge length and axial load subjected to near-fault earthquakes

For all cases studied in Fig. 11, the length of the plastic hinge is estimated using the procedure described previously. As can be seen in the Figure, the length of the plastic hinge is nearly constant at low axial loads ($P \leq 0.2P_o$). At low axial loads, the obtained l_p values are equal to 0.55 h. Starting at an axial load of approximately $0.2P_o$, l_p increases with increasing axial loads. The l_p estimate of 0.55h (Fig. 11) can be compared with 0.4h recommended by Park and Priestley [31] and 0.5h recommended by Paulay and Priestley [32] and 0.25h by Bae and Bayrak [23]. The differences observed in the l_p estimates can be attributed to the displacement components used to estimate the l_p values. Bae and Bayrak [23] only considered the flexural displacements as the strains experienced by compression bars were obtained from the moment-curvature relationships. It is important to note that for the calculation of l_p in the present paper, not only flexural deformations were considered but also deformations due to bar slip and shear deformations were calculated.

In the Bae and Bayrak experimental tests [23], the critical section in the columns shifts away from the face of the stub, due to additional confinement effects provided by the stub. Because of the additional confinement provided by the stub to adjacent sections, sections within a distance of approximately 0.25h from the stub remain nearly undamaged. Therefore, in order to estimate the length of the plastic hinge region, (in which columns are expected to dissipate significant amounts of inelastic energy by undergoing large inelastic deformations), Bae and Bayrak suggested subtracting an amount of 0.25h from the overall length in which compressive reinforcing bar strains greater than the yield strain are calculated. Adding the term of 0.25h and considering deformations due to bar slip and shear deformations, Bae and Bayrak's results have been shown to be in good agreement with the experimental tests.

7.2 Height-depth ratio (H/h)

In order to investigate the influence of H/h on the length of plastic hinge, 716 nonlinear dynamic analyses were conducted. The square RC columns with various levels of axial loads and height over depth ratios subjected to the 7 selected records were studied. At this stage of the parametric study, the longitudinal reinforcement ratio was kept constant at ρ_l = 0.01. The results of the analyses are summarized in Fig. 12 and Fig 13.

Adding the term of 0.25 h to the Bae and Bayrak experimental tests [23] and considering deformations resulting from bar slip and shear deformations helps in realising a good agreement with the experimental tests.

As is seen in Fig. 13, l_p increases as H/h increases for a given axial load level. At low axial loads ($\approx 0.2P_0$), the increases observed in l_p with increasing H/h are insignificant. For a given H/h, the l_p increases as axial loads increase. The increases in l_p observed at small H/h ($2 < H/h < 3$) are less pronounced than those observed at large H/h values. The comparison between results in this study and past studies show that plastic hinge length in RC columns subjected to combined effect of near-fault vertical and horizontal ground motions higher than plastic hinge length in RC columns subjected to far-fault earthquakes [24].

8 Proposed expression for plastic hinge length

Several factors influence the length of plastic hinge, such as:

1 level of axial load;

2 moment gradient;

3 the value of shear stress in the plastic hinge region;

4 the amount and mechanical properties of longitudinal and transverse reinforcement;

5 strength of concrete;

Tab. 2. Predicted length of plastic hinge for different levels of axial load subjected to near-fault earthquakes

Axial Load	Kobe	Northridge	Landers	Erzican	Morgan Hill	Imperial Valley	Gazli	Average
0	0.48	0.48	0.52	0.48	0.49	0.47	0.48	0.48
0.1	0.49	0.49	0.53	0.5	0.51	0.48	0.47	0.49
0.2	0.56	0.51	0.54	0.51	0.52	0.50	0.59	0.53
0.3	0.74	0.71	0.74	0.75	0.69	0.69	0.73	0.72
0.4	0.87	0.82	0.79	0.99	0.85	1.09	0.89	0.9
0.5	1.04	0.99	1.19	1.20	1.10	1.19	1.19	1.13
0.6	1.31	1.20	1.35	1.37	1.25	1.28	1.33	1.30
0.7	1.49	1.37	1.54	1.55	1.46	1.44	1.48	1.47
0.8	1.74	1.59	1.68	1.70	1.69	1.67	1.65	1.67

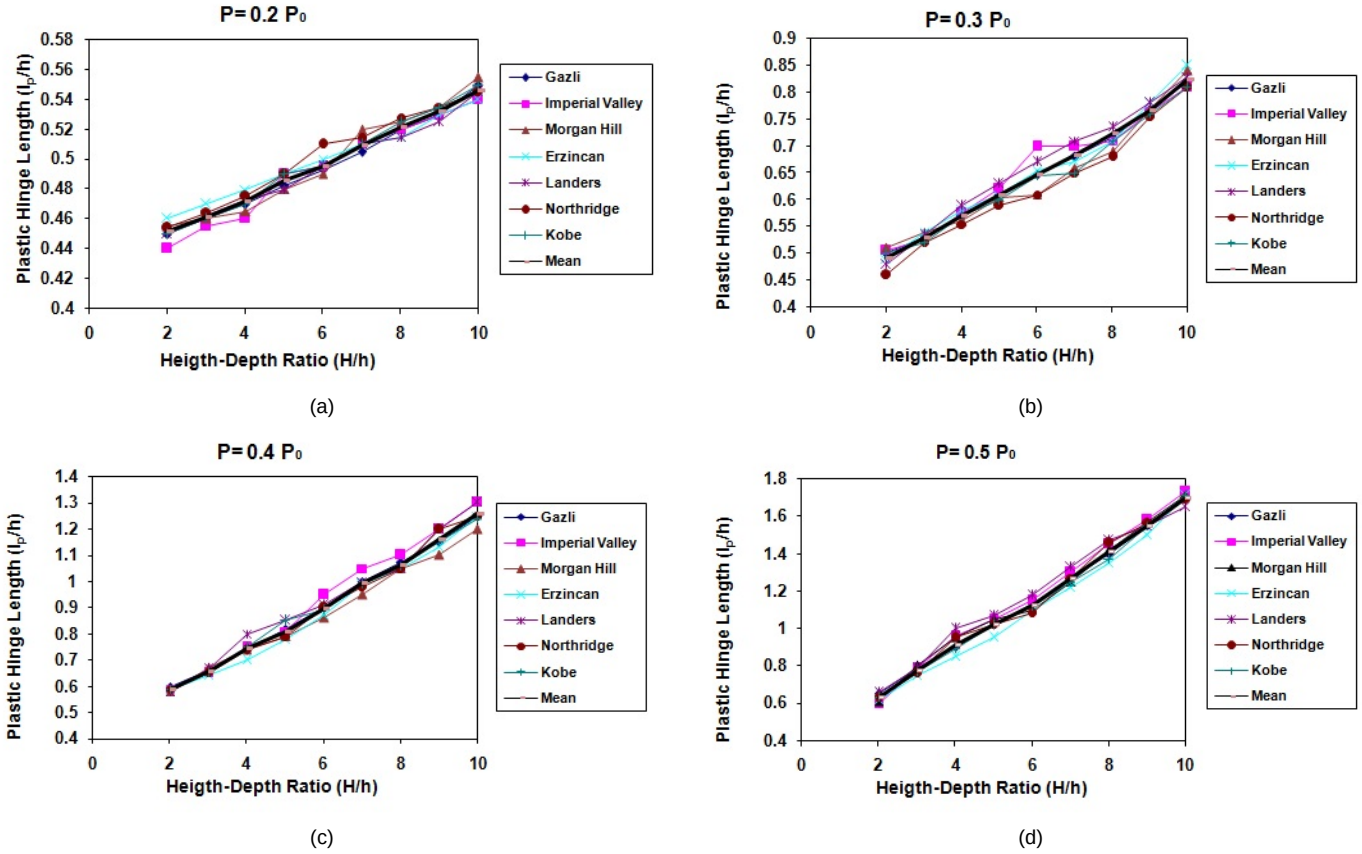

Fig. 12. Relationship between plastic hinge length and height-depth ratio for various levels of axial load subjected to near-fault earthquakes

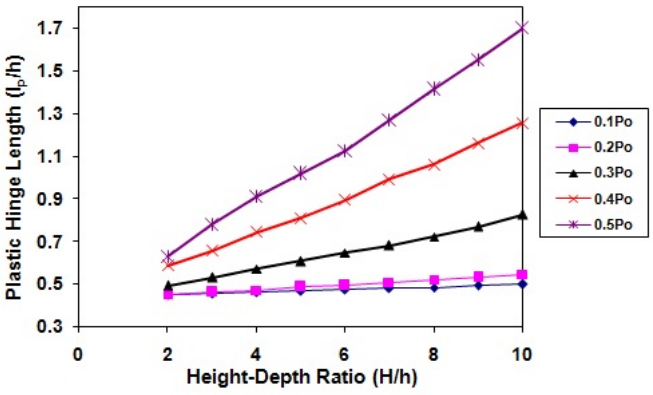

Fig. 13. Relationship between plastic hinge length (average) and height-depth ratio for various levels of axial load subjected to near-fault earthquakes

6 level of confinement provided in the potential plastic hinge zone; and

7 different characteristics of earthquakes.

The simplified equations available in the literature do not contain all, or even most, of the aforementioned factors. Hence, large variations exist in the values of plastic hinge length calculated using these empirical equations, as shown clearly in Fig. 3. Baker, in his work, considered most of the parameters affecting plastic hinge length. He found that the contribution of the longitudinal reinforcement effect is not considerable.

Bae and Bayrak [23] presented an expression for the estimation of plastic hinge length of RC columns. Compared to other equations presented by other researchers, this equation includes the level of axial force (P/P_0), height over depth ratio (H/h), and amount of longitudinal steel (A_s/A_g). However, this equation presents a problem, in that only flexural displacements were considered in the proposed analysis.

Based on the numerical results obtained in this study, the following equations are suggested for the estimation of plastic hinge length in RC columns subjected to the combined effect of near-fault vertical and horizontal ground motions:

$$\begin{array}{ll} \frac{l_p}{h} = 0.85\left[1 + 0.45\,\frac{P}{P_0}\right]\left(\frac{H}{h}\right)^{0.2} \cdot k & for\ P/P_0 > 0.2 \\ \frac{l_p}{h} = 0.55 & for\ P/P_0 \le 0.2 \end{array} \quad (7)$$

In the above, h is the overall depth of column, P is the applied axial load, P_0 is the nominal axial load capacity, H is the distance from critical section to the point of contraflexure and $k = 0.65$ when $f'_c = 32.5$ MPa; and $k = 0.85$ when $f'_c = 12.5$ MPa and $k = 0.85 - 0.01\,(f'_c - 12.5)$, where $32.5\,\text{MPa} < f'_c < 12.5\,\text{MPa}$.

These equations compare favourably with the calculated values in this paper and measured values reported in the Kumagai and Kawashima [30] and Bae and Bayrak experimental work [23].

To investigate the accuracy of above equations, the plastic hinge length of four RC columns specimens that were tested by Kumagai and Kawashima [30], are estimated using various expressions and compared with the measured plastic hinge length in the Table 3.

The result of comparison show that by means of the proposed equations, reasonable estimations can be made of the plastic hinge length of RC columns under the high and low axial load levels and combined effect of near-fault vertical and horizontal ground motions. Also, the result of comparison of proposed equations and some past equations show that using some equations may overestimate the plastic hinge length of RC columns and vice versa; but the proposed equations can calculate the plastic hinge length of RC columns reasonably, in both high level and low level of axial load.

9 Conclusions

In earthquake engineering, plastic hinge is a type of energy damping device allowing plastic rotation of a rigid column connection. Plastic hinges form at the maximum moment regions of RC columns. The determination of the length of plastic hinge is a critical step in predicting the lateral load versus drift response of columns. As it is difficult to estimate the plastic hinge length using analytical methods, it is often estimated based on experimental data or empirical equations. This paper presents the results of a comprehensive numerical study on the length of plastic hinge in RC columns. Hundreds of time-history analyses have been performed in order to evaluate the plastic hinge lengths, and the results are presented. The following conclusions can be drawn based on the results:

1 The numerical results show good correlation with the available experimental results and indicate the usefulness of the nonlinear finite element as a powerful tool to study the behaviour of different types of RC elements subjected to the combined effect of near-fault vertical and horizontal ground motions.

2 The above mentioned method of calculating the plastic hinge length gives good correlation with the experimental values.

3 The results show that potential l_p specified by many code is not satisfactory for columns supporting high axial loads and combined effect of near-fault vertical and horizontal ground motions and can even be non-conservative in some cases. It is suggested that the length of the region in which closely-spaced ties are used is increased from $1.0\,h$ to $1.5\,h$ from the joint face.

4 Analytical models for columns analysed under high axial loads exhibit longer plastic hinges than those analysed under low axial loads.

5 The plastic hinge length in RC columns subjected to combined effect of near-fault vertical and horizontal ground motions is higher than that plastic hinge length in RC columns subjected to far-fault earthquakes, possibly because, vertical ground motions are high-frequency motions and the increase in axial force demands with a decrease in vertical period (increase in frequency) is in accordance with the high-frequency characteristic of vertical ground motions.

6 The following equation, developed in this research, provide a further insight into the understanding of the plastic hinge length of RC members and allow a better estimation of the plastic hinge length of RC members under combined effect of near-fault vertical and horizontal ground motions:

$$\begin{array}{ll} \frac{l_p}{h} = 0.85\left[1 + 0.45\,\frac{P}{P_0}\right]\left(\frac{H}{h}\right)^{0.2} \cdot k & forP/P_0 > 0.2 \\ \frac{l_p}{h} = 0.55 & forP/P_0 \le 0.2 \end{array}$$

Tab. 3. Estimated plastic hinge length by various expressions

Specimen	Baker	Corley	Mattock	Park et al.	Paulay & Priestley	Sheikh & Khoury	Measured	Proposed equation
Case 1	0.57h	0.49h	0.70h	0.40h	0.80h	1.00h	1.1h	1.04h
Case 2	0.62h	0.52h	0.80h	0.40h	0.96h	1.00h	1.19h	1.24h
Case 3	0.60h	0.49h	0.70h	0.40h	0.72h	1.00h	0.68h	0.69h
Case 4	0.52h	0.49h	0.70h	0.40h	0.72h	1.00h	0.65h	0.69h

References

1 **Chang SW, Bray JD, Seed RB**, *Engineering implications of ground motions from the Northridge earthquake*, Bulletin of the Seismological Society of America, **86**(1B), (1996), 270–288.

2 **Abrahamson NA, Silva WJ**, *Empirical Response Spectral Attenuation Relations for Shallow Crustal Earthquakes*, Seismological Research Letters, **68**(1), (1997), 94–127, DOI 10.1785/gssrl.68.1.94.

3 *Iranian Code of Practice for Seismic Resistant Design of Buildings (3rd Edition)*, Building and Housing Research Center; Tehran, Iran, 2005.

4 **Kazinczy G**, *Experiments with Clamped Beams*, Betonszemle, **2**(4, 5, 6), (1914), 68-71, 83-87, 101-104.

5 **Kheyroddin A, Mortezaei A**, *The effect of element size and plastic hinge characteristics on nonlinear analysis of RC frames*, Iranian Journal of Science & Technology, Transaction B, **32**(B5), (2008), 451–470.

6 **Iványi M**, *The model of the interactive plastic hinge*, Periodica Polytechnica Civil Engineering, **29**(3-4), (1985), 123–146.

7 **Park R, Paulay T**, *Reinforced Concrete Structures*, John Wiley and Sons; New York, USA, 1975, DOI 10.1002/9780470172834.

8 **Broderick BM, Elnashai AS**, *Analysis of the failure of interstate 10 freeway ramp during the Northridge earthquake of 17 January 1994*, Earthquake Engineering & Structural Dynamics, **24**(2), (1995), 189–208, DOI 10.1002/eqe.4290240205.

9 **Abdelkareem KH, Machida A**, *Effect of vertical motion of earthquake on failure mode and ductility of RC bridge piers*, 12th World Conference on Earthquake Engineering, In: Effect of vertical motion of earthquake on failure mode and ductility of RC bridge piers; Canada, 2000.

10 **Bozorgnia YM, Campbell KW**, *The vertical-to-horizontal response spectral ratio and tentative procedures for developing simplified V/H and vertical design spectra*, Journal of Earthquake Engineering, **8**(3), (2004), 175–207, DOI 10.1080/13632460409350486.

11 **Kunnath SH, Zhao H**, *Effects of near-fault vertical accelerations on highway bridge columns*, 25th US - Japan Bridge Engineering Workshop, In: Effects of near-fault vertical accelerations on highway bridge columns; Tsukuba Japan, October 19-21, 2009.

12 **Kunnath SK, Erduran E, Chai YH, Yashinsky M**, *Effect of Near-Fault Vertical Ground Motions on Seismic Response of Highway Overcrossings*, Journal of Bridge Engineering, **13**(3), (2008), 282–290, DOI 10.1061/(ASCE)1084-0702(2008)13:3(282).

13 **Hashemi BH, Abbassi E**, *Rational suggestions for vertical component requirement in 2800 Iranian standard for near-fault areas*, Journal of Seismology and Earthquake Engineering, **10**(4), (2009), 189–194.

14 **Matsuzaki H, Kawashima K**, *Effect of high frequency component predominant vertical ground motions on the seismic performance of bridge*, Journal of Earthquake Engineering, **30**, (2009), 499–506.

15 **Kim SJ, Holub CJ, Elnashai AS**, *Analytical Assessment of the Effect of Vertical Earthquake Motion on RC Bridge Piers*, Journal of Structural Engineering, **137**(2), (2011), 252–260, DOI 10.1061/(ASCE)ST.1943-541X.0000306.

16 **Baker ALL**, *Ultimate load theory applied to the design of reinforced and prestressed concrete frames*, Concrete Publications Ltd; London, 1956.

17 **Baker ALL, Amarakone AMN**, *Plastic Inelastic hyper-static frame analysis*, International symposium on the flexural mechanics of reinforced concrete, In: Plastic Inelastic hyper-static frame analysis; Miami USA, November 1964, pp. 85–142.

18 **Riva P, Cohn MZ, Gill WD**, *Engineering approach to nonlinear analysis of concrete structures*, Journal of Structural Division ASCE, **116**, (1990), 2162–2186.

19 **Corley WG**, *Rotational capacity of reinforced concrete beams*, Journal of the Structural Division ASCE, **92**(ST5), (1966), 121–146.

20 **Mattock AH**, *Rotational capacity of hinging regions in reinforced concrete beams*, International symposium on the flexural mechanics of reinforced concrete, In:; Miami USA, November 1964, pp. 143–181.

21 **Sawyer HA**, *Design of concrete frames for two failure stages*, International symposium on the flexural mechanics of reinforced concrete, In: Design of concrete frames for two failure stages; Miami USA, November 1964, pp. 405–431.

22 **Fernandes C, Melo J, Varum H, Costa A**, *Cyclic behavior of a two-span RC beam built with plain reinforcing bars*, Periodica Polytechnica Civil Engineering, **55**(1), (2011), 21–29, DOI 10.3311/pp.ci.2011-1.03.

23 **Bae S, Bayrak O**, *Plastic hinge length of reinforced concrete columns*, ACI Structural Journal, **105**(3), (2008), 290–300.

24 **Mortezaei A, Ronagh HR**, *Plastic hinge length of reinforced concrete columns subjected to both far-fault and near-fault ground motions having forward directivity*, The Structural Design of Tall and Special Buildings, **22**(12), (2013), 903–926, DOI 10.1002/tal.729.

25 **Mortezaei A, Ronagh HR, Kheyroddin A, Ghodrati Amiri G**, *Effectiveness of modified pushover analysis procedure for the estimation of seismic demands of buildings subjected to near-fault earthquakes having forward directivity*, The Structural Design of Tall and Special Buildings, **20**(6), (2011), 679–699, DOI 10.1002/tal.553.

26 **Iwan WD, Moser MA, Peng CY**, *Some observations on strong-motion earthquake measurements using a digital accelerograph*, Bulletin of the Seismological Society of America, **75**, (1985), 1225–1246.

27 **Iwan WD, Chen XD**, *Near-field ground motion data from the Landers earthquake*, 10th European Conference on Earthquake Engineering, In: Near-field ground motion data from the Landers earthquake; Vienna, Austria, 1994.

28 **Boore D**, *Effect of Baseline Corrections on Displacements and Response Spectra for Several Recordings of the 1999 Chi-Chi, Taiwan, Earthquake*, Bulletin of the Seismological Society of America, **91**(5), (2001), 1199–1211, DOI 10.1785/0120000703.

29 **Boore D, Stephens CD, Joyner WB**, *Comments on Baseline Correction of Digital Strong-Motion Data: Examples from the 1999 Hector Mine, California, Earthquake*, Bulletin of the Seismological Society of America, **92**(4), (2002), 1543–1560, DOI 10.1785/0120000926.

30 **Kumagai Y, Kawashima K**, *Effect of high frequency vertical ground motions on the restoring force of reinforced concrete bridge piers*, Journal of Structural Engineering, **132**(1), (2010), 112–122.

31 **Park R, Priestley MJN, Gill WD**, *Ductility of square-confined concrete columns*, Journal of Structural Division ASCE, **108**(ST4), (1982), 929–950.

32 **Paulay T, Priestley MJN**, *Seismic Design of Reinforced Concrete and Masonry Buildings*, John Wiley and Sons; New York, USA, 1992, DOI 10.1002/9780470172841.